Journal of the Serbian Chemical Society
JSCS-info@shd.org.rs • www.shd.org.rs/JSCS
J. Serb. Chem. Soc. *82* (4) 437–447 (2017)
JSCS–4979
UDC 620.1+66.017+549.517.2:678.686:531.004.12+536.6
Original scientific paper

Influence of hematite nanorods on the mechanical properties of epoxy resin

GORDANA BOGDANOVIĆ[1], TIJANA S. KOVAČ[2], ENIS S. DŽUNUZOVIĆ[3]*, MILENA ŠPÍRKOVÁ[4], PHILLIP S. AHRENKIEL[5] and JOVAN M. NEDELJKOVIĆ[6]

[1]Faculty of Engineering, University of Kragujevac, Sestre Janjić 6, 34000 Kragujevac, Serbia, [2]Innovation Center, Faculty of Technology and Metallurgy, University of Belgrade, Karnegijeva 4, Belgrade 11120, Serbia, [3]Faculty of Technology and Metallurgy, University of Belgrade, Karnegijeva 4, 11120 Belgrade, Serbia, [4]Institute of Macromolecular Chemistry AS CR, v.v.i., Heyrovského nám. 2, 16206 Prague 6, Czech Republic, [5]South Dakota School of Mines and Technology, 501 E. Saint Joseph St., Rapid City, SD 57701, USA and [6]Institute of Nuclear Sciences Vinča, University of Belgrade, P. O. Box 522, 11000 Belgrade, Serbia

(Received 7 July 2016, revised 25 January, accepted 30 January 2017)

Abstract: The mechanical properties of nanocomposites obtained by incorporation of fairly uniform hematite nanorods (α-Fe_2O_3 NRs) into epoxy resin were studied as a function of the content of the inorganic phase. A thorough microstructural characterization of the α-Fe_2O_3 NRs and the nanocomposites was performed using transmission electron microscopy (TEM) and atomic force microscopy (AFM). The TEM measurements revealed rod-like morphology of the nanofiller with a uniform size distribution (8.5 nm×170 nm, diameter×length). High-magnification TEM and AFM measurements indicated agglomeration of α-Fe_2O_3 NRs embedded in the epoxy resin. Stress at break, strain at break, elastic modulus and tensile toughness of the nanocomposites were compared with the data obtained for pure epoxy resin. Significant influence of nanofiller on the mechanical properties of epoxy resin, as well as on the glass transition temperature, could be noticed for samples with low contents of the inorganic phase (up to 1 wt. %).

Keywords: nanocomposites; thermosetting resin; mechanical measurements; differential scanning calorimetry.

INTRODUCTION

Epoxy resins have found wide applications in adhesives, coatings, electronic encapsulants, medical devices, and optical and structural components due to their superior properties.[1] However, the brittle nature of most epoxy resins has driven extensive research into the influences of different fillers on their mechanical pro-

* Corresponding author. E-mail: edzunuzovic@tmf.bg.ac.rs
doi: 10.2298/JSC160707017B

perties. Hitherto, a variety of fillers, such as rubber particles, glass beads, thermoplastic particles, inorganic particles, as well as combinations of these materials have been used in order to improve mechanical properties of epoxy resins.[2]

Recent developments in nanoscience, including synthetic procedures for size and shape control of various nanoparticles, have presented possibilities to prepare epoxy-based nanocomposites with significantly improved mechanical properties. Several studies indicated that the modulus, strength and toughness could be simultaneously increased with the addition of nanoscale fillers.[2–9] Nanoparticles can significantly alter the mechanical properties of a polymer matrix, even at low concentrations, due to their high surface to volume ratio and consequential small inter-particle distance. Incorporation of nanorods into a polymer matrix can improve the mechanical properties of the matrix that cannot be achieved using the same amount of a spherical nanofiller. This effect becomes more pronounced with increasing aspect ratio of rod-like nanofillers.[10–12] Interaction between nanofillers and polymer chains alters the mobility of the polymer chains, which is indicated by a change in the glass transition temperature.[13] Most studies concerning inorganic nanoscale fillers and epoxy resins have been conducted using commercially available spherical nanoparticles, such as SiO_2,[3,5,8,9,13–16] Al_2O_3,[17–20] TiO_2,[21] hybrid TiO_2–SiO_2,[22] ZrO_2[23] and SiC.[24] On the other hand, there is a lack of information about the influences of zero-dimensional (0D) and one-dimensional (1D) inorganic nanofillers[25] on the mechanical properties of epoxy resins, with the exception of graphene,[26] carbon nanofibers,[27–29] and carbon nanotubes.[30] To date, ferric oxide particles of different sizes and morphologies, 0D (spherical and cubic) and 1D (rod-like), have been used to improve the thermo-mechanical properties of thermoplastic polymers (polystyrene[31–33] and poly(methyl methacrylate)[34–36]). To the best of our knowledge, only the influence of commercially available spherical Fe_2O_3 particles (diameter in the size range from 20 to 60 nm) on the mechanical properties of epoxy resins has been reported in literature.[20]

In this study, uniform hematite nanorods (α-Fe_2O_3 NRs) with average diameter of 8.5 nm and aspect ratio of about 20 were introduced into epoxy resin with the view of improving the mechanical properties of the composite systems. Mechanical performance of nanocomposites (stress at break, strain at break, elastic modulus and tensile toughness) with low contents of inorganic phase (up to 1 wt. %) was compared with the mechanical properties of pure epoxy resin. The morphology of the obtained nanocomposites was studied using different microscopy techniques, while the influence of the content of α-Fe_2O_3 NRs on the glass transition temperature (T_g) was studied using differential scanning calorimetry (DSC).

EXPERIMENTAL

Synthesis of uniform hematite nanorpds (α-Fe_2O_3 NRs)

Powder consisting of α-Fe_2O_3 NRs was obtained by courtesy of Dr. Milena Marinović-Cincović. The synthetic procedure and structural characterization of the α-Fe_2O_3 NRs are described in a previous work.[35] Briefly, a dispersion consisting of α-Fe_2O_3 NRs was obtained by forced hydrolysis of $FeCl_3$ solution in a manner similar to the method developed by Matijević.[37] Thus, 100 mL of 5.4 M NaOH was added to 100 mL of 2 M $FeCl_3$, and the solution was stirred at room temperature for 15 min. Subsequently, the solution was heated to 100 °C and the temperature was maintained for 8 days. The α-Fe_2O_3 NRs were recovered by centrifugation, washed several times with water and dried in a vacuum oven. As expected, the XRD analysis indicated that synthesized powder was α-Fe_2O_3 with a corundum crystal structure, known for weakly ferromagnetic or superparamagnetic behavior depending on particle size.[31]

Preparation of α-Fe_2O_3/epoxy nanocomposites

A commercially available epoxy resin, CHS-Epoxy 210 X 75, was used as the polymer matrix, which was cured with Epikure 3115 X 70 hardener, using a weight ratio of 100:35. Nanocomposites with different contents of α-Fe_2O_3 NRs were obtained according to the same procedure. The required amount of α-Fe_2O_3 NRs was dispersed in 3.9 g of xylene (isomeric mixture) , added to 6 g of CHS-Epoxy 210 X 75, and mixed in an ultrasonic bath for 10 min. Then, the corresponding amount of curing agent, Epicure 3115 X 70, was added. The obtained mixture was additionally mixed in an ultrasonic bath for 10 min and then poured into a Teflon dumb-bell-shaped mould. The curing of the so-prepared samples was performed at room temperature for 21 days. The declared content of inorganic phase was calculated with respect to the total mass of epoxy resin and curing agent. A pure epoxy resin sample, without α-Fe_2O_3 nanorods, was prepared under the same experimental conditions.

Characterization of the α-Fe_2O_3/epoxy nanocomposites

The morphology and particle size distribution of the α-Fe_2O_3 powders as well as the morphology of the α-Fe_2O_3/epoxy nanocomposites were analyzed using a JEM-2100 LaB6 transmission electron microscope (TEM) operated at 200 kV. In addition, the topography and heterogeneity “bulk” relief from the nano to micrometer levels was realized by AFM. The nanocomposite sheets were measured after previous freeze-fracture at liquid nitrogen temperature. An atomic force microscope (Dimension Icon, Bruker), equipped with an SSS-NCL probe, Super Sharp SiliconTM-SPM-Sensor (NanoSensorsTM Switzerland; spring constant 35 N m^{-1}, resonant frequency ≈170 kHz) was used for the analysis. Measurements were performed under ambient conditions using the tapping mode AFM technique. AFM scans covered areas from 1×1 μm^2 to 50×50 μm^2.

Mechanical measurements of the pure epoxy resin and the α-Fe_2O_3/epoxy nanocomposites were performed on a Galdabini 1890 (Quasar 5) tensile testing machine with nominal capacity of 5 kN. The dumbbell-type specimens were 2.50±0.05 mm thick and 4 mm wide at the neck. For stress–strain measurements, the crosshead speed was 20 mm min^{-1}. The presented values for the stress at break, the strain at break and the Young’s elastic modulus are the average of at least five runs. The tensile toughness of examined nanocomposites was determined from the area underneath the stress–strain curves.

Differential scanning calorimetry (DSC) was performed at a heating rate of 20 °C min^{-1} under a nitrogen atmosphere using a Perkin Elmer DSC-2 instrument.

RESULTS AND DISCUSSION

The shape and size distribution of α-Fe_2O_3 particles were estimated using TEM. A typical TEM image at low magnification of the α-Fe_2O_3 NRs is shown in Fig. 1A. It could be noticed that the α-Fe_2O_3 NRs had a tendency to array themselves parallel to each other and to form bundle-like aggregates. The corresponding size distribution histograms for the diameter and length (Figs. 1B and C, respectively) were determined on a population of over 250 particles. The average diameter and length of α-Fe_2O_3 NRs were found to be 8.5 and 170 nm, respectively, and consequently the aspect ratio of rod-like particles was 20. The standard deviations of the diameter and length were found to be 2 and 75 nm, respectively. Based on the particle size distribution data, it is clear that it is more difficult to control length than the diameter of α-Fe_2O_3 NRs. It is well known that the ability to control length of nanorods decreases with increasing aspect ratio, while, on the other hand, their tendency to array parallel to each other and to form bundle-like aggregates increases.[34]

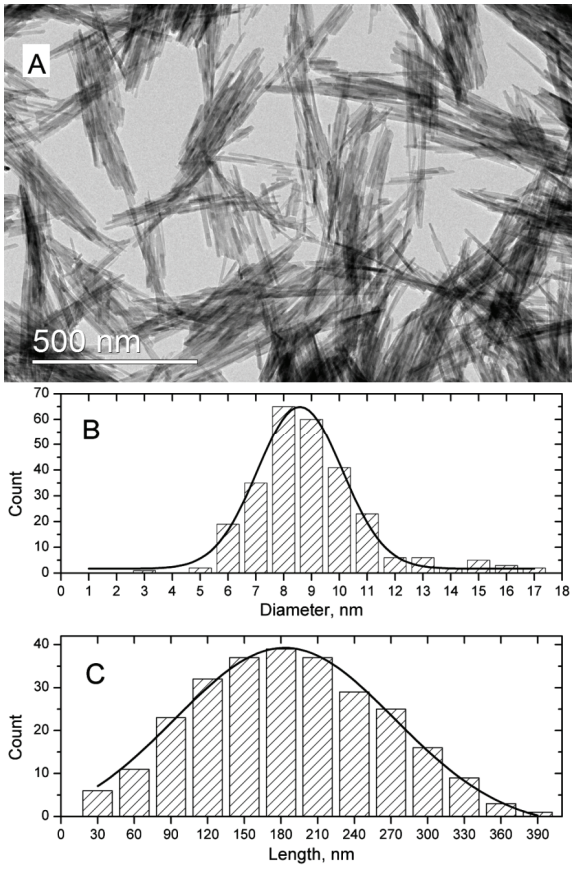

Fig. 1. A typical TEM image of the α-Fe_2O_3 NRs (A) and the corresponding size distributions of the diameter and length (B and C, respectively).

The morphology of the α-Fe_2O_3/epoxy composites was studied using AFM and TEM measurements. The AFM phase image of the epoxy filled with 0.5 wt. % of inorganic phase is shown in Fig. 2A. It is clear that an epoxy-rich phase and inorganic-rich phases existed after the addition of α-Fe_2O_3 NRs, indicating a high degree of agglomeration of the nanofiller. Additional TEM measurements at high magnification (Fig. 2B) confirmed that the α-Fe_2O_3 NRs formed bundle-like aggregates in the epoxy matrix, although some individual nanorods were also visible. It should be kept in mind that no attempt was made to improve compatibility of epoxy resin and α-Fe_2O_3 NRs by surface modification.

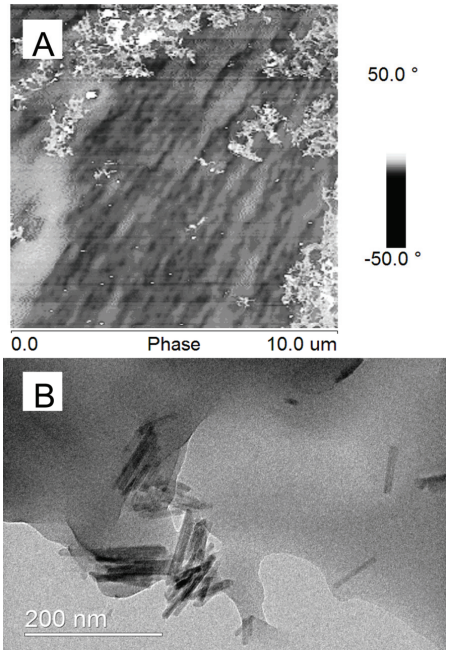

Fig. 2. AFM (A) and TEM (B) images of the α-Fe_2O_3/epoxy nanocomposite with 0.5 wt. % of inorganic phase.

The glass transition temperatures (T_g) of the pure epoxy resin and the α-Fe_2O_3/epoxy nanocomposites were determined by DSC. The DSC thermograms of the examined samples are shown in Fig. 3. The values of the glass transition temperature were taken as the midpoint of the glass transition event and are listed in Table I. Except for the sample with the highest content of α-Fe_2O_3 NRs (1.0 wt. %), all the other composite samples had a lower glass transition temperature than that of the pure epoxy resin. The composite sample with 1.0 wt % of α-Fe_2O_3 NRs has the same T_g as the pure epoxy resin. The ratio of epoxy resin to hardener was constant for all the prepared samples, which were treated in the same way. Moreover, no post-curing reactions were observed by DSC. This indicates that the maximal degree curing was reached in the examined samples and that all samples have the same crosslinking density. The obtained results indicate

that the observed reduction of the T_g of nanocomposites was caused by diffusion of free volume holes towards the filler–polymer interfaces.[38,39] This reduction of T_g is directly related to the ratio of the surface the α-Fe_2O_3 filler/volume of epoxy matrix. In the sample with 1.0 wt. % of α-Fe_2O_3 NRs, agglomeration of the nanoparticles and formation of aggregates occurred. This drastically reduced the interfacial area between the α-Fe_2O_3 NRs and the epoxy matrix, making the influence of the filler on the glass transition temperature negligible. These results are contrary to the results obtained by Dudić and co-workers.[40] They examined the electrical properties of nanocomposites prepared from hematite nanorods and epoxy resin. The calculation of the T_g of the examined samples was based on the results obtained by conductivity measurements. Thus, the estimated values of the T_g indicated that incorporation of hematite nanorods shifted the T_g of the epoxy matrix towards higher temperatures compared to the pure epoxy resin. The increase in the T_g was explained by the reduced mobility of the epoxy segments in the presence of high specific surface fillers. The curing agent was a low molar mass diamine while, in the present case, the curing agent was polyaminoamide. According to Dudić and co-workers, a layer with reduced mobility was formed at the interface of the polymer/nanoparticles during curing, because the diamine could easily reach the surface of the nanoparticles. In the present study, this layer was not formed because the polyaminoamide hardener could not reach the filler surface so easily during the curing reaction and this is a possible reason for the contradictory results.

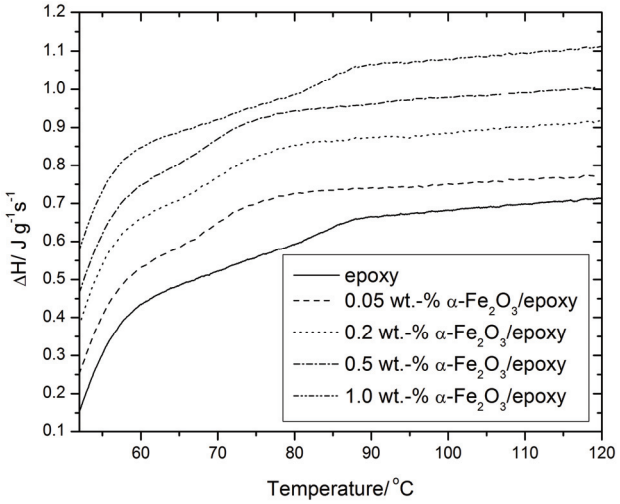

Fig. 3. DSC curves of pure epoxy resin and of the α-Fe_2O_3/epoxy nanocomposites.

Typical stress–strain curves of pure epoxy resin and the nanocomposites with different α-Fe_2O_3 NRs loadings are shown in Fig. 4. Data for the stress and

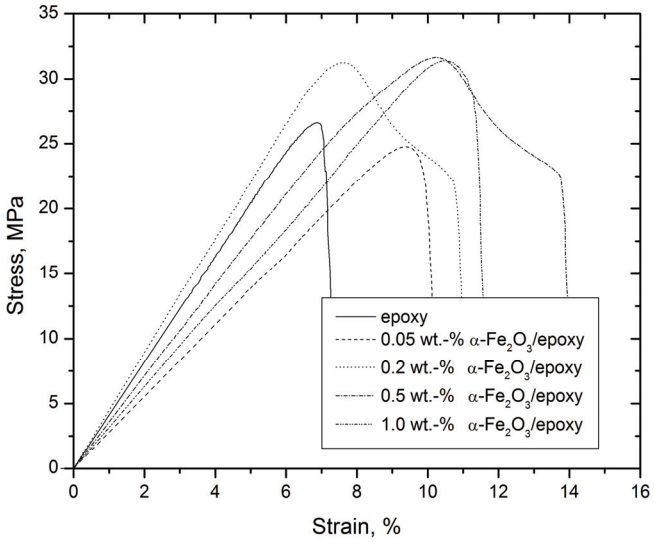

Fig. 4. Stress–strain curves of the pure epoxy resin and the α-Fe_2O_3/epoxy nanocomposites.

strain at break, and the Young's modulus were collected as a function of the content of α-Fe_2O_3 NRs and are presented in Table I. The stress and strain at break values, and the Young's modulus of pure epoxy resin were 26.3 MPa, 7.0 % and 410 MPa, respectively. The values for the stress at break, strain at break and elastic modulus for a nanocomposite depends on the content of inorganic phase. For example, a continuous increase in the strain at break with increasing content of inorganic phase could be observed with the exception of the sample with the highest content of inorganic phase (1.0 wt. % of α-Fe_2O_3 NRs). The strain at break for sample with 0.5 wt. % of α-Fe_2O_3 NRs was higher by 49 % compared to that for the pure epoxy resin. The strain at break of all nanocomposite samples was larger than the strain at break of the pure epoxy sample. This results in a larger area under stress–strain curves, indicating increasing toughness of the epoxy matrix. It is well known that the main problem in the applications of epoxy resins is the brittle nature of epoxy resins, and hence, numerous strategies have been used to improve their toughness.[41–44] One of these strategies is the usage of different nanoscale fillers.[45–51] Tensile toughness data of the prepared α-Fe_2O_3/ /epoxy nanocomposites and pure epoxy resin, calculated as the area under the stress–strain curve, are given in Table I. The increase of tensile toughness from 1.06 MJ m^{-3} for pure epoxy resin to 2.79 MJ m^{-3} for the nanocomposite with 0.5 wt. % of α-Fe_2O_3 NRs could be noticed, while a further increase of filler content caused a decrease of the tensile toughness (2.02 MJ m^{-3} for the nanocomposite filled with 1.0 wt. % of α-Fe_2O_3 NRs) due to filler aggregation. Dudić and co- -workers[40] also showed that the fracture surface of the pure epoxy resin was

relatively smooth and featureless while a pronounced roughness was observed in the case of the α-Fe_2O_3 nanorods/epoxy resin nanocomposite, indicating that the α-Fe_2O_3 nanorods promoted ductile deformation of the epoxy matrix.

TABLE I. Stress at break, strain at break, Young's elastic modulus, glass transition temperature (T_g) and tensile toughness (U_T) of the pure epoxy resin and the α-Fe_2O_3/epoxy nanocomposites

Content of α-Fe_2O_3 NRs, wt. %	Stress at break, MPa	Strain at break, %	Elastic modulus, MPa	T_g / °C	U_T / MJ m^{-3}
0.0	26.3	7.0	410	80	1.06
0.05	23.0	9.8	277	72	1.40
0.2	21.9	10.7	447	71	2.15
0.5	22.5	13.7	357	71	2.79
1.0	29.7	11.1	316	80	2.02

The 2.63-fold increase in the tensile toughness upon incorporation of 0.5 wt. % of unmodified α-Fe_2O_3 NRs into the epoxy resin is at least comparable to or better than that attained by other nanofillers. For example, incorporation of 1.0 wt. % of TiO_2 increased the tensile toughness 1.70-fold,[21] 1.0 wt. % of Gr/ /Fe@Fe_2O_3 increased the tensile toughness more than 2-fold,[27] 15.5 wt. % of clay increased the tensile toughness by about 1.75 times,[48] 1.0-wt. % of Fe@FeO increases the tensile toughness more than 1.5-fold,[49] while incorporation of 13.4 wt. % of nanosilica increased the fracture toughness of epoxy resin by 2.40 times.[50]

On the other hand, the stress at break values for the nanocomposites with low contents of inorganic phase (≤0.5 wt. %) were slightly lower compared to that for the pure epoxy resin, while the value for the nanocomposite with the highest concentration of α-Fe_2O_3 NRs (1.0 wt. %) was 13 % larger than that for the pure epoxy resin (29.7 and 26.3 MPa, respectively). The values of the Young's modulus of the nanocomposites were lower compared to that of the pure epoxy resin, except the sample containing 0.2 wt. % of α-Fe_2O_3 NRs.

According to the obtain results, the most likely toughening mechanism is plastic void growth. The repulsive interactions at the interface between the α-Fe_2O_3 NRs nanofiller and the epoxy matrix facilitate debonding of the nanofiller and formation of voids around the α-Fe_2O_3 NRs, which allows plastic deformation of the matrix.

The yield point could be observed from the stress–strain curves of the nanocomposite samples with 0.2 and 0.5 wt. % of α-Fe_2O_3 NRs. The yield stress was about 32 MPa for these samples, but at the different elongations (a higher value for the sample with the higher content of inorganic phase). Most likely, this effect is a consequence of alignment of the α-Fe_2O_3 NRs together with the polymer chains when yielding occurred.

The obtained results indicate a significant influence of the 1D nanofiller on the mechanical properties of the epoxy matrix even when the content of inorganic phase was smaller than 1 wt. %. However, there is a lack of information in literature concerning the performance of epoxy-based nanocomposites with embedded ferric-oxide nanoparticles. Recently, Reis *et al.*[20] showed that reinforcement of polymer mortars with spherical Fe_2O_3 nanoparticles in the size range from 20 to 60 nm led to an increase of their elastic and fracture properties. Although the shape and concentration range of the nanofiller differed in the case of published data and this study, there is a reasonable good agreement in observed effects.

CONCLUSIONS

Epoxy-resin-based nanocomposites were prepared by embedding fairly uniform ferric oxide nanorods in order to understand better the influence of 1D nanofillers on the mechanical properties of polymer matrices. The tensile properties (stress at break, strain at break, Young's elastic modulus and tensile toughness) and the glass transition temperature of the epoxy resins were significantly altered in the presence of α-Fe_2O_3 NRs at the low concentration levels ($\leq$1.0 wt. %). The tendency of inorganic nanoparticles with rod-like morphology to form bundle-like aggregates was enhanced in the surrounding media of different polarity. This is the main obstacle that limits reinforcement of polymer matrices with 1D nanofillers. For this reason, future work will be focused on the improvement of the compatibility of epoxy resin and α-Fe_2O_3 NRs.

Acknowledgements. Financial support for this study was granted by the Ministry of Education, Science and Technological Development of the Republic of Serbia (Project No. 45020). The AFM analysis was realized within the project 13-06700S (Czech Science Foundation).

И З В О Д

УТИЦАЈ ХЕМАТИТНИХ НАНОШТАПИЋА НА МЕХАНИЧКА СВОЈСТВА ЕПОКСИДНЕ СМОЛЕ

ГОРДАНА БОГДАНОВИЋ[1], ТИЈАНА С. КОВАЧ[2], ЕНИС С. ЦУНУЗОВИЋ[3], MILENA ŠPÍRKOVÁ[4], PHILLIP S. AHRENKIEL[5] и ЈОВАН М. НЕДЕЉКОВИЋ[6]

[1]Факултет техничких наука Универзитета у Крагујевцу, Сестре Јањић 6, 34000 Крагујевац, [2]Иновациони центар, Технолошко–металуршки факултет Универзитета у Београду, Карнегијева 4, 11120 Београд, [3]Технолошко-металуршки факултет Универзитета у Београду, Карнегијева 4, 11120 Београд, [4]Institute of Macromolecular Chemistry AS CR, v.v.i., Heyrovského nám. 2, 16206 Prague 6, Czech Republic, [5]South Dakota School of Mines and Technology, 501 E. Saint Joseph St., Rapid City, SD 57701, USA и [6]Институт за нуклеарне науке Винча, Универзитет у Београду, п. пр. 522, 11000 Београд

Механичка својства нанокомпозита, добијених додатком хематита у облику штапића нанометарских димензија (α-Fe_2O_3 NRs) у епоксидну смолу, проучавана су у функцији садржаја неорганске фазе. Микроструктурна карактеризација α-Fe_2O_3 NRs и нанокомпозита извршена је коришћењем трансмисионе електронске микроскопије (TEM) и помоћу микроскопа атомских сила (AFM). На основу TEM резултата показано је да ко-

ришћено нанопунило има штапићасту морфологију са униформном расподелом величине (пречник × дужина, 8,5 nm × 170 nm). TEM и AFM мерења су показала да долази до агломеризације α-Fe_2O_3 NRs у епоксидној смоли. Вредности напона и деформације при кидању, модула еластичности и жилавости нанокомпозита, су упоређене са вредностима добијеним за чисту епоксидну смолу. Утврђено је да додатак врло мале количине α-Fe_2O_3 NRs (до 1 мас. %) има значајан утицај на механичка својства и на температуру остакљивања епоксидне смоле.

(Примљено 7. јула 2016, ревидирано 25. јануара, прихваћено 30. јануара 2017)

REFERENCES

1. B. Ellis, *Chemistry and technology of epoxy resins*, Blackie Academic & Professional, New York, 1993
2. B. Wetzel, P. Rosso, F. Haupert, K. Friedrich, *Eng. Fract. Mech*. **73** (2006) 2375
3. A. J. Kinloch, R. D. Mohammed, A. C. Taylor, C. Eger, S. Sprenger, D. Egan, *J. Mater. Sci.* **40** (2005) 5083
4. J. T. Han, K. Cho, *Macromol. Mater. Eng*. **290** (2005) 1184
5. G. Ragosta, M. Abbate, P. Musto, G. Scarinzi, L. Mascia, *Polymer* **46** (2005) 10506
6. J. T. Han, K. Cho, *J. Mater. Sci.* **41** (2006) 4239
7. A. J. Kinloch, A. C. Taylor, *J. Mater. Sci.* **41** (2006) 3271
8. P. Rosso, L. Ye, K. Friedrich, S. Sprenger, *J. Appl. Polym. Sci.* **100** (2006) 1849
9. H. Zhang, Z. Zhang, K. Friedrich, C. Eger, *Acta Mater.* **54** (2006) 1833
10. M. J. A. Hore, R. J. Composto, *Macromolecules* **47** (2014) 875
11. R. Scotti, L. Conzatti, M. D'Arienzo, B. Di Credico, L. Giannini, T. Hanel, P. Stagnaro, A. Susanna, L. Tadiello, F. Morazzoni, *Polymer* **55** (2014) 1497
12. A. M. Mihut, A. Sáncchez-Ferrer, J. Crassous, L. Ackerman Hirschi, R. Mezzenga, H. Dietsch, *Polymer* **54** (2013) 4194
13. E. Bugnicourt, J. Galy, J. F. Gerard, H. Barthel, *Polymer* **48** (2007) 1596
14. C. Chen, R. S. Justice, D. W. Schaefer, J. W. Baur, *Polymer* **49** (2008) 3805
15. Y. T. Bia, Z. J. Lia, W. Lianga, *Polym. Adv. Technol*. **25** (2014) 173
16. H. Gu, J. Guo, H. Wei, *J. Mater. Chem., C* **3** (2015) 8152
17. B. Wetzela, F. Hauperta, M. Q. Zhang, *Compos. Sci. Technol.* **63** (2003) 2055
18. Z. Guo, T. Pereira, O. Choi, Y. Wang, H. T. Hahn*, J. Mater. Chem.* **16** (2006) 2800
19. L. M. McGrath, R. S. Parnas, S. H. King, J. L. Schroeder, D. A. Fischer, J. L. Lenhart, *Polymer* **49** (2008) 999
20. J. M. L. Reis, D. C. Moreira, L. C. S. Nunes, L. A. Sphaier, *Compos. Struct*. **93** (2011) 3002
21. A. Chatterjee, M. S. Islam, *Mat. Sci. Eng., A-Struct*. **487** (2008) 574
22. A. Omrania, S. Afsarb, M. A. Safarpour, *Mater. Chem. Phys*. **122** (2010) 343
23. R. Medina, F. Haupert, A. K. Schlarb, *J. Mater. Sci.* **43** (2008) 3245
24. R. M. Rodgers, H. Mahfuz, V. K. Rangari, N. Chisholm, S. Jeelani, *Macromol. Mater. Eng.* **290** (2005) 42
25. J. N. Tiwari, R. N. Tiwari, K. S. Kim, *Prog. Mater. Sci.* **57** (2012) 724
26. X. Zhang, O. Alloul, Q. He, J. Zhu, M. J. Verde, Y. Li, S. Wei, Z. Guo, *Polymer* **54** (2013) 3594
27. J. Zhang, C. H. Wang, H. Niu, A. Gestos, T. Lin, X. Wang, *Compos., A* **55** (2013) 45
28. H. Gu, J. Guo, H. Wei, S. Guo, J. Liu, Y. Huang, M. A. Khan, X. Wang, D. P. Young, S. Wei, Z. Guo, *Adv. Mater.* **27** (2015) 6277
29. Q. Zhang, L. Liu, D. Jiang, X. Yan, Y. Huang, Z. Guo, *J. Compos. Mater.* **49** *(*2015) 2877

30. M. Abdalla, D. Dean, M. Theodore, J. Fielding, E. Nyairo, G. Price, *Polymer* **51** (2010) 1614
31. V. Djoković, J. M. Nedeljković, *Macromol. Rapid Comm.* **21** (2000) 994
32. J. Kuljanin, M. Marinović-Cincović, S. Zec, M. I. Čomor, J. M. Nedeljković, *J. Mater. Sci. Lett.* **22** (2003) 253
33. M. Marinović-Cincović, Z. V. Šaponjić, V. Djoković, S. K. Milonjić, J. M. Nedeljković, *Polym. Degrad. Stabil.* **91** (2006) 313
34. M. Marinović-Cincović, M. Č. Popović, M. M. Novaković, J. M. Nedeljković, *Polym. Degrad. Stab.* **92** (2007) 70
35. E. Džunuzović, M. Marinović-Cincović, K. Jeremić, J. Vuković, J. Nedeljković, *Polym. Degrad. Stab.* **93** (2008) 73
36. E. Džunuzović, M. Marinović-Cincović, K. Jeremić, J. Nedeljković, *Polym. Degrad. Stab.* **94** (2009) 701
37. E. Matijević, *Langmuir* **2** (1986) 12
38. V. M. Boucher, D. Cangialosi, A. Alegría, J. Colmenero, I. Pastoriza-Santos, L. M. Liz--Marzan, *Soft Matter* **7** (2011) 3607
39. J. G. Curro, R. R. Lagasse, *Macromolecules* **15** (1982) 1621
40. D. Dudić, M. Marinović-Cincović, J. M. Nedeljković, V. Djoković, *Polymer* **49** (2008) 4000
41. K. P. Unnikrishnan, E. T. Thachil, *Des. Monomers Polym*. **9** (2006) 129
42. T. Liu, X. Geng, Y. Nie, R. Chen, Y. Meng, X. Li, *RSC Adv.* **4** (2014) 30250
43. L. F. Low, A. Abu Bakar, *J. Compos. Mater.* **45** *(* 2011) 2287
44. R. A. Pearson, A. F. Yee, *Polymer* **34** (1993) 3658
45. Z. Wang, F. Liu, W. Liang, L. Zhou*, J. Reinf. Plast. Comp*. **32** (2013) 1224
46. P. K. Ghosh, K. Kumar, N. Chaudhary, *Compos., B* **77** (2015) 139.
47. Q. H. Le, H. C. Kuan, J. B. Dai, I. Zaman, L. Luong , J. Ma, *Polymer* **51** (2010) 4867
48. J. H. Park, S. C. Jana, *Polymer* **44** (2003) 2091
49. J. Zhu, S. Wei, J. Ryu, L. Sun, Z. Luo, Z. Guo, *ACS Appl. Mater. Inter.* **2** (2010) 2100
50. B. B. Johnsen, A. J. Kinloch, R. D. Mohammed, A. C. Taylor, S. Sprenger, *Polymer* **48** (2007) 530
51. E. Bugnicourt, J. Galy, J. F. Gérard, H. Barthel, *Polymer* **48** (2007) 1596.